COMMUNICATIONS IN NUMERICAL METHODS IN ENGINEERING

EVALUATION OF SOME ERROR ESTIMATORS FOR THE FOUR-NODED LAGRANGIAN QUADRILATERAL

A. C. A. RAMSAY and H. SBRESNY

School of Engineering, University of Exeter, North Park Road, Exeter, EX4 4QF U.K.

SUMMARY

A comparative study of error estimators using a patch recovery scheme with those using simple nodal averaging is made for the four-noded Lagrangian quadrilateral element through two plane stress elasticity problems. It is demonstrated that error estimators using a patch recovery scheme are generally more effective and have an estimated stress field that is closer to the exact one than those using simple nodal averaging.

1. INTRODUCTION

Over recent years a number of error estimators for estimating the error in a standard displacement method finite element approximation have been proposed. Of these methods those that estimate the error through the construct of a continuous *estimated stress field* have received much attention[1,2]. For these error estimators the estimated stress field is achieved by interpolating a set of unique nodal stresses over the element with the same basis functions used to interpolate displacements in the original analysis. Different methods for achieving the unique nodal stresses then result in different estimated stress fields and, therefore, different estimates of the error. This paper compares error estimators for which the unique nodal stresses are achieved by simple nodal averaging with those that use a patch recovery scheme[2]. Numerical results for two problems in plane elasticity are reported for the standard four-noded Lagrangian element.

2. ESTIMATING THE ERROR WITH CONTINUOUS ESTIMATED STRESS FIELDS

The continuous estimated stress field $\tilde{\boldsymbol{\sigma}}$ is constructed from the discontinuous finite element stress field $\boldsymbol{\sigma}_h$ by interpolating a set of unique nodal stresses $\boldsymbol{s}$ over the element using the same basis functions as those used for the interpolation of the displacements in the original analysis:

$$\tilde{\boldsymbol{\sigma}} = \overline{N} s \tag{1}$$

This process is shown for a single component of stress in Figure 1.

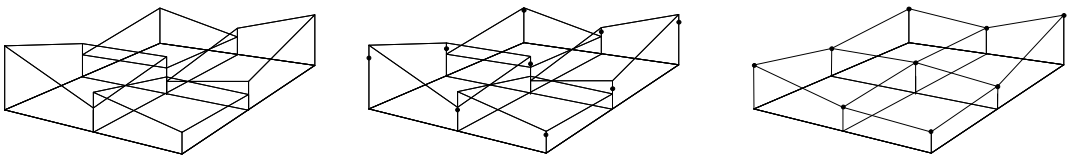

(a) Discontinuous $\boldsymbol{\sigma}_h$ (b) Unique nodal stresses (c) Continuous $\tilde{\boldsymbol{\sigma}}$

Figure 1. Transforming from a discontinuous $\boldsymbol{\sigma}_h$ to a continuous $\tilde{\boldsymbol{\sigma}}$ by interpolating unique nodal stresses $\boldsymbol{s}$ over an element with the basis functions for the element

The error in the finite element stress field $\boldsymbol{\sigma}_e$ is the difference between the true stress field $\boldsymbol{\sigma}$ and the finite element stress field $\boldsymbol{\sigma}_h$:

$$\boldsymbol{\sigma}_e = \boldsymbol{\sigma} - \boldsymbol{\sigma}_h \tag{2}$$

In cases where the true stress field is unknown it is replaced by the estimated stress field $\tilde{\boldsymbol{\sigma}}$ (the tilde is used to indicate estimated quantities) and the estimated error in the finite element stress field $\tilde{\boldsymbol{\sigma}}_e$ is defined as:

$$\tilde{\boldsymbol{\sigma}}_e = \tilde{\boldsymbol{\sigma}} - \boldsymbol{\sigma}_h \tag{3}$$

These distributions of error can be integrated over an element to form a single number representing the error in that element. The *strain energy of the error* U_e for element *i* is:

$$U_{ei} = \frac{1}{2}\int_V \sigma_{ei}^T \varepsilon_{ei} dV \tag{4}$$

and, for the estimated error, the *strain energy of the estimated error* $\tilde{U}_e$ for element *i* is:

$$\tilde{U}_{ei} = \frac{1}{2}\int_V \tilde{\sigma}_{ei}^T \tilde{\varepsilon}_{ei} dV \tag{5}$$

where $\boldsymbol{\varepsilon}_e$ and $\tilde{\boldsymbol{\varepsilon}}_e$ represent strain fields corresponding to $\boldsymbol{\sigma}_e$ and $\tilde{\boldsymbol{\sigma}}_e$ respectively and *V* represents the volume of element *i*.

For a mesh of *ne* elements the total error is simply the summation of all elemental contributions:

$$U_e = \sum_{i=1}^{ne} U_{ei} \tag{6}$$

and

$$\tilde{U}_e = \sum_{i=1}^{ne} \tilde{U}_{ei} \tag{7}$$

The effectivity of an error estimator is then measured by the *effectivity ratio* β which is defined as:

$$\boldsymbol{\beta} = \frac{\tilde{U}_e}{U_e} \tag{8}$$

The closer the effectivity ratio is to unity, the more effective the error estimator.

The philosophy of error estimation presented above follows that given in Reference 3 in which strain energy quantities, as opposed to energy norm quantities, are used to define the effectivity of an error estimator. The effectivity *index* θ of Reference 1 is related to the effectivity *ratio* of equation (8) as $\theta = \sqrt{\beta}$.

Because of the integral nature of the quantities involved in the effectivity ratio, it is possible for different estimated stress fields to yield the same effectivity ratio. In order to distinguish between such estimated stress fields a further quantity is introduced. The *error in the estimated stress field* $\hat{\boldsymbol{\sigma}}$ is defined as the difference between the true stress field $\boldsymbol{\sigma}$ and the estimated stress field $\tilde{\boldsymbol{\sigma}}$:

$$\hat{\boldsymbol{\sigma}} = \boldsymbol{\sigma} - \tilde{\boldsymbol{\sigma}} \tag{9}$$

The *strain energy of the error in the estimated stress field* $\hat{U}$ for element *i* is then:

$$\hat{U}_i = \frac{1}{2}\int_V \hat{\sigma}_i^T \hat{\varepsilon}_i dV \tag{10}$$

and, for a mesh of *ne* elements:

$$\hat{U} = \sum_{i=1}^{ne} \hat{U}_i \tag{11}$$

The smaller the value of $\hat{U}$ the closer the estimated stress field is to the true stress field.

3. CO-ORDINATE SYSTEMS FOR THE PATCH RECOVERY SCHEME

In the patch recovery scheme as proposed by Zienkiewicz and Zhu[2] the unique nodal stresses $\boldsymbol{s}$ are obtained for each node by fitting a polynomial stress surface σ_p through the superconvergent (stress) points surrounding a particular node in a least squares manner. This idea is shown schematically in Figure 2. For the element under consideration there is a single superconvergent point at the isoparametric centre of the element[4].

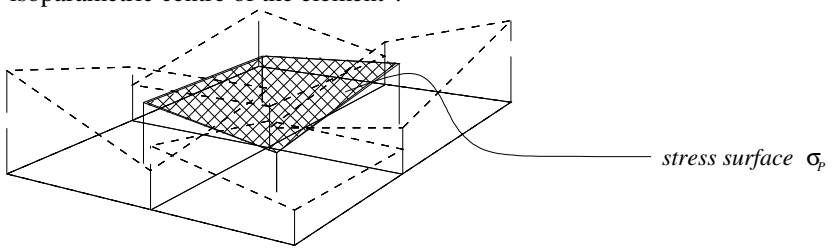

Figure 2. Patch recovery scheme for a patch of four elements

The stress surface for a particular component of stress is defined as:

$$\boldsymbol{\sigma}_p = \boldsymbol{P}\boldsymbol{a} \tag{12}$$

where $\boldsymbol{P}$ is a row vector of polynomial terms and the parameters $\boldsymbol{a}$ are obtained by a least-square fit of the stress surface to the set of superconvergent stress points in the patch considered.

The terms used in the row vector $\boldsymbol{P}$ could be those corresponding to those used in the basis functions i.e. the incomplete bi-linear polynomial terms $\boldsymbol{P}=\lfloor 1, x, y, xy \rfloor$ or they could be those that form a complete linear polynomial i.e. $\boldsymbol{P}=\lfloor 1, x, y \rfloor$ where x and y are ordinates in the global Cartesian co-ordinate system. In their original paper[2] Zienkiewicz and Zhu suggest that the incomplete bi-linear polynomial terms may give better results and should therefore be used.

In a subsequent paper[5] it was recognised that the use of the global co-ordinate system could result in numerical difficulties in evaluating the parameters $\boldsymbol{a}$. In order to overcome this problem the use of a locally normalized Cartesian co-ordinate system $(\bar{x}, \bar{y})$, as shown in Figure 3, was recommended[5]. However, recent studies[6] have shown that although this modification is sufficient to overcome the numerical difficulties occurring when using a complete linear polynomial stress surface, it is not sufficient to overcome the problems associated with the orientation of the patch in the global co-ordinate system when the incomplete bi-linear polynomial is used. These difficulties are fully explained in Reference 6 and in this article the parent patch concept is developed in which the stress surface is defined in terms of the ordinates of a curvilinear co-ordinate system (ξ, η) as shown in Figure 3. Use of the parent patch concept avoids the problems associated with the orientation of the patch.

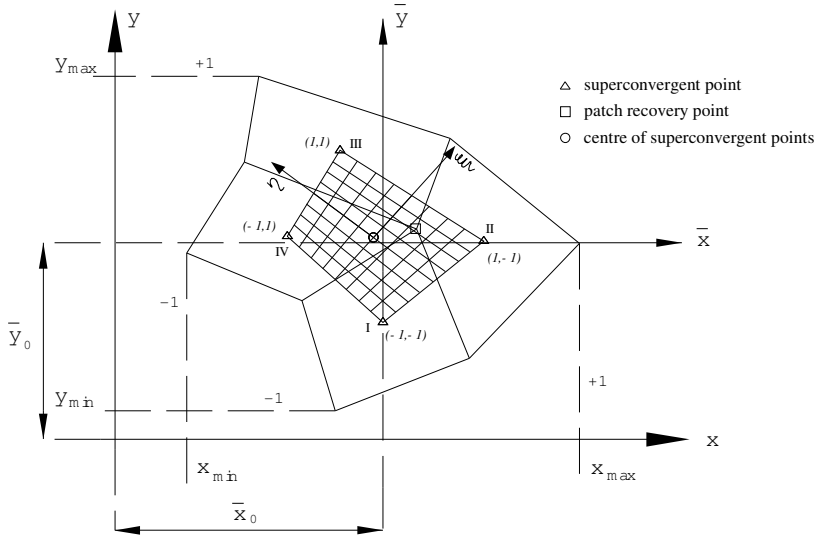

Figure 3. The parent patch and associated co-ordinate systems

4. THE ERROR ESTIMATORS

Different methods for obtaining the unique nodal stresses $\boldsymbol{s}$ will result in different estimated stress fields $\tilde{\boldsymbol{\sigma}}$ and, therefore different values for β and $\widehat{U}$. In this paper we shall compare three error estimators that use a patch recovery scheme with one that uses simple nodal averaging of the finite element stresses at a node. These error estimators are now defined.

Error estimator EE2: the unique nodal stresses are determined by simple nodal averaging[1] of the finite element nodal stresses recovered at the nodes through bi-linear extrapolation from 2x2 Gauss points[7]. This error estimator was discussed in detail in Reference 3.

Error estimator EEL: the unique nodal stresses are obtained from a patch recovery scheme using a locally normalized *Cartesian* co-ordinate system[5] and a *complete linear polynomial* definition for the stress surface.

Error estimator EEb: the unique nodal stresses are obtained from a patch recovery scheme using a locally normalized *Cartesian* co-ordinate system[5] and an *incomplete bi-linear polynomial* definition for the stress surface.

Error estimator EEp: the unique nodal stresses are obtained from a patch recovery scheme using a locally normalized *curvilinear* co-ordinate system[6] and an *incomplete bi-linear polynomial* definition for the stress surface.

For error estimators which use a patch recovery scheme the nodal stresses at the boundary of the model are recovered by extrapolation from the nearest appropriate internal patch as recommended in References 2 and 10 and shown schematically in Figure 4. The integration of all strain energy quantities is performed using 2x2 Gauss quadrature which is exact for parallelogram shaped elements.

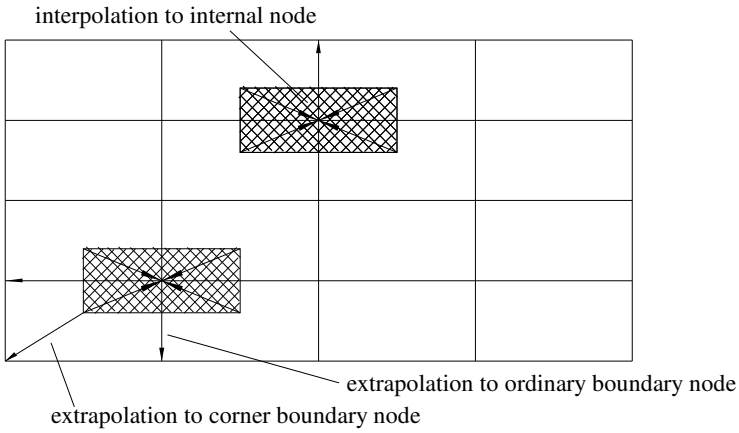

Figure 4. Recovery of boundary stresses through use of an internal patch

5. NUMERICAL STUDIES

The performance of these error estimators will be evaluated through two plane stress elasticity problems which have known analytical solutions. The integral quantities β and $\hat{U}$ will be compared and the pointwise quality of the estimated stress field $\tilde{\boldsymbol{\sigma}}$ examined. The models were restrained against rigid body motion and loaded with consistent nodal forces.

5.1. Problem 1

Figure 5 shows a rectangular continuum subjected to static boundary conditions consistent with a linear stress field.

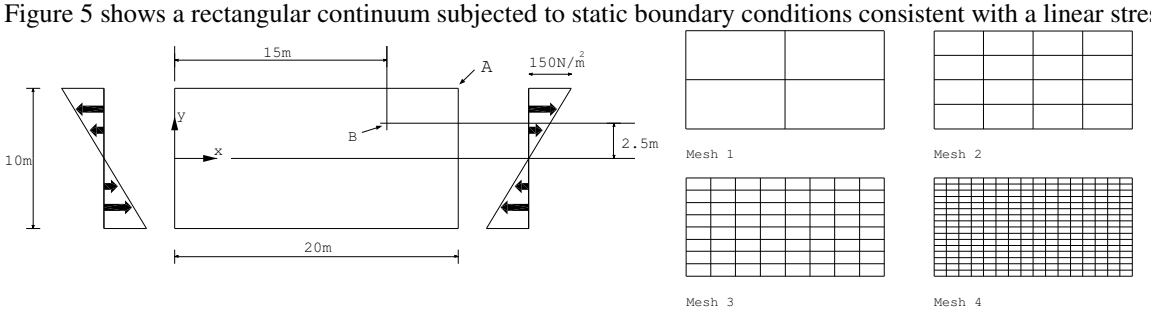

(a) The problem (b) The meshes

Figure 5. Problem 1

For this problem the analytical solution in stress is:

$$\begin{aligned} \sigma_x &= 30\,y \\ \sigma_y &= 0 \\ \tau_{xy} &= 0 \end{aligned} \tag{13}$$

With a Young's Modulus of $E = 210\,N/m^2$, a Poisson's Ratio of $\nu = 0.3$ and a material thickness of $t = 0.1m$ the exact strain energy is $U = 2500/7\,Nm$.

The quality of the recovered stresses will be considered at Points A & B in the model (see Figure 5). Since the exact values of the σ_y- and τ_{xy}- components of stress are zero at these points only the σ_x-component of the stress will be considered. The σ_x- component of the recovered stress at Points A & B are tabulated in Table I and the convergence of the error in the recovered stress is shown in Figure 6. In this figure the gradient of selected curves *n* is indicated and a

triangular wedge indicating the superconvergent rate of convergence (*n*=2) is also shown. The quantities β and $\hat{U}$ are shown in Table VI.

Table I. Convergence of σ_x- component of the recovered stress at Points A and B for Problem 1. For Point A the exact value is $\sigma_x = 150\, N/m^2$ whilst for Point B the exact value is $\sigma_x = 75\, N/m^2$

		Point A				Point B			
Mesh	h	$\tilde{\sigma}_2$	$\tilde{\sigma}_L$	$\tilde{\sigma}_b$	$\tilde{\sigma}_p$	$\tilde{\sigma}_2$	$\tilde{\sigma}_L$	$\tilde{\sigma}_b$	$\tilde{\sigma}_p$
1	10/1	111.70	106.43	106.43	106.43	\	\	\	\
2	10/2	135.60	136.61	134.39	134.39	69.62	68.47	68.47	68.47
3	10/4	143.92	144.70	142.29	142.29	73.48	73.30	73.30	73.30
4	10/8	147.05	147.39	146.10	146.10	74.57	74.56	74.56	74.56

In Table I the *h* is taken as the *x*-dimension of an element.

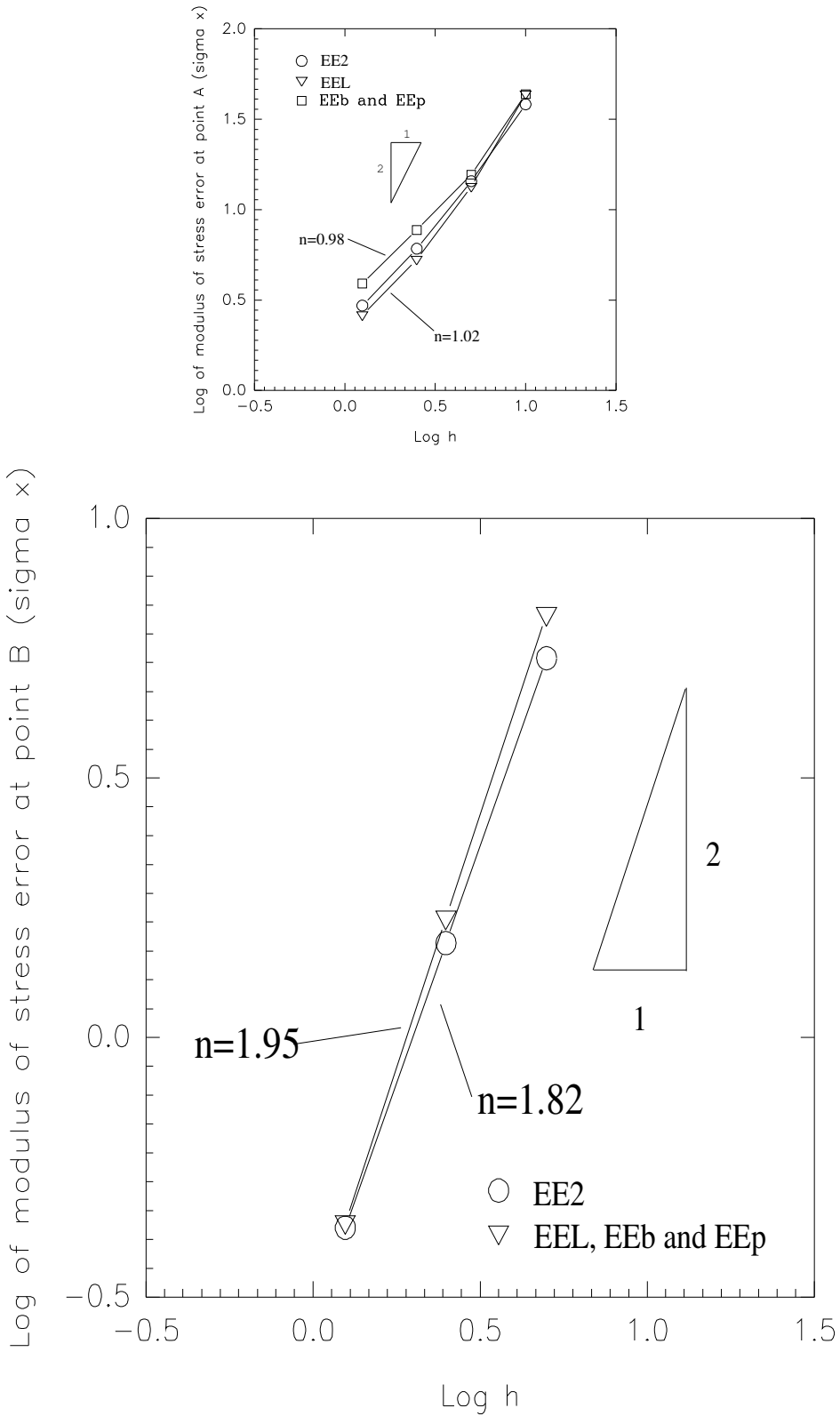

(a) Point A (b) Point B

Figure 6. Convergence characteristics of error in recovered stress for Problem 1

5.2. Problem 2

In this problem the classical case of an unstressed circular hole centred in an infinite membrane under a uniform tension of amplitude σ_∞ in the *x*-direction is considered. A finite portion of this membrane is considered as shown in Figure 7a and a symmetric quarter of this finite portion is modelled as shown in Figure 7b.

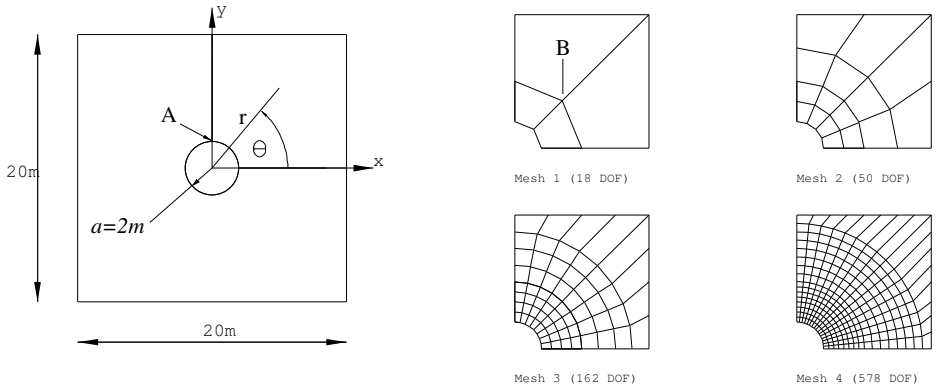

(a) The geometry (b) The meshes

Figure 7. Problem 2

For this problem the analytical solution in stress[8] is given as:

$$\begin{aligned}
\sigma_x &= \sigma_\infty \{1-\frac{a^2}{r^2}(\frac{3}{2}\cos 2\theta+\cos 4\theta)+\frac{3}{2}\frac{a^4}{r^4}\cos 4\theta\} \\
\sigma_y &= \sigma_\infty \{0-\frac{a^2}{r^2}(\frac{1}{2}\cos 2\theta-\cos 4\theta)-\frac{3}{2}\frac{a^4}{r^4}\cos 4\theta\} \\
\tau_{xy} &= \sigma_\infty \{0-\frac{a^2}{r^2}(\frac{1}{2}\sin 2\theta+\sin 4\theta)+\frac{3}{2}\frac{a^4}{r^4}\sin 4\theta\}
\end{aligned} \tag{14}$$

For a Young's Modulus of $E = 10\times10^6\ N/m^2$, a Poisson's Ratio of $\nu = 0.25$ and a material thickness of $t = 0.01m$ the exact strain energy is $U = 5.188448459\,Nm$ and is accurate to the number of digits quoted.

For this problem there is a stress concentration in the σ_x- component of the stress at Point A ($r = 2m, \theta = \pi/2$) and the way in which this component of the recovered stress converges at this point, is shown in Table II. For the internal point, Point B ($r = 5m, \theta = \pi/4$) all three components of the exact stress are non-zero and the components of the recovered stresses for this point are shown, respectively, in Tables, III, IV and V.

Table II. Convergence of σ_x- component of the recovered stress at Point A for Problem 2.

The exact value is $\sigma_x = 30,000\ N/m^2$.

Mesh	σ_h	$\tilde{\sigma}_2$	$\tilde{\sigma}_L$	$\tilde{\sigma}_b$	$\tilde{\sigma}_p$
1	23004.2	20539.2	10884.6	13191.6	17979.5
2	26973.0	25269.4	17585.2	22776.8	23065.2
3	29522.9	28681.2	23942.2	26270.3	26386.8
4	30325.9	30012.9	27813.2	28451.1	28468.5

Table III. Convergence of σ_x- component of the recovered stress at Point B for Problem 2.

The exact value is $\sigma_x = 11216.02\, N/m^2$.

Mesh	σ_h	$\tilde{\sigma}_2$	$\tilde{\sigma}_L$	$\tilde{\sigma}_b$	$\tilde{\sigma}_p$
1	9762.57	9477.41	10016.48	10094.42	10016.80
2	10829.13	10734.18	10684.81	20687.06	10684.87
3	11118.59	11090.96	11044.98	10924.94	11045.89
4	11206.11	11198.52	11168.79	8313.12	11168.16

Table IV. Convergence of σ_y- component of the recovered stress at Point B for Problem 2.

The exact value is $\sigma_y = -1216.02\, N/m^2$.

Mesh	σ_h	$\tilde{\sigma}_2$	$\tilde{\sigma}_L$	$\tilde{\sigma}_b$	$\tilde{\sigma}_p$
1	-296.46	-309.10	-63.50	-69.85	-63.49
2	-912.96	-879.23	-714.62	-2366.91	-714.66
3	-1111.68	-1100.11	-1053.74	-1061.11	-1053.96
4	-1189.42	-1186.14	-1172.12	-773.15	-1172.34

Table V. Convergence of τ_{xy}- component of the recovered stress at Point B for Problem 2.

The exact value is $\tau_{xy} = -800.02\, N/m^2$.

Mesh	σ_h	$\tilde{\sigma}_2$	$\tilde{\sigma}_L$	$\tilde{\sigma}_b$	$\tilde{\sigma}_p$
1	-784.60	-701.17	-716.11	-694.50	-716.21
2	-770.92	-752.55	-740.15	-3439.73	-739.96
3	-782.20	-777.39	-784.89	-843.67	-784.75
4	-790.58	-789.29	-796.26	-449.37	-796.81

Note that in Tables II - V σ_h is the nodal average of the finite element stresses evaluated directly at the node.

For this problem, where uniform mesh refinement is not employed, the various recovered stresses considered are simply plotted against the mesh number as shown in Figure 8.

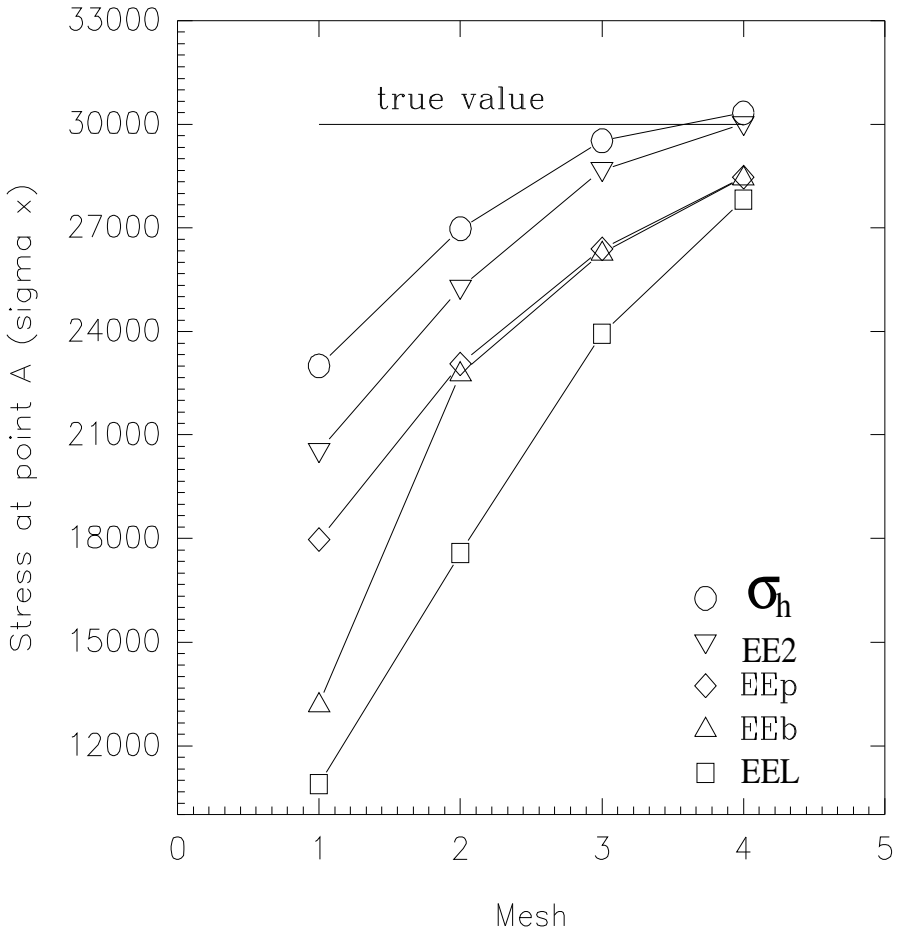
33000
30000
27000
24000
21000
18000
15000
12000
Stress at point A (sigma x)
true value
0
1
2
3
4
5
Mesh
σh
EE2
EEp
EEb
EEL

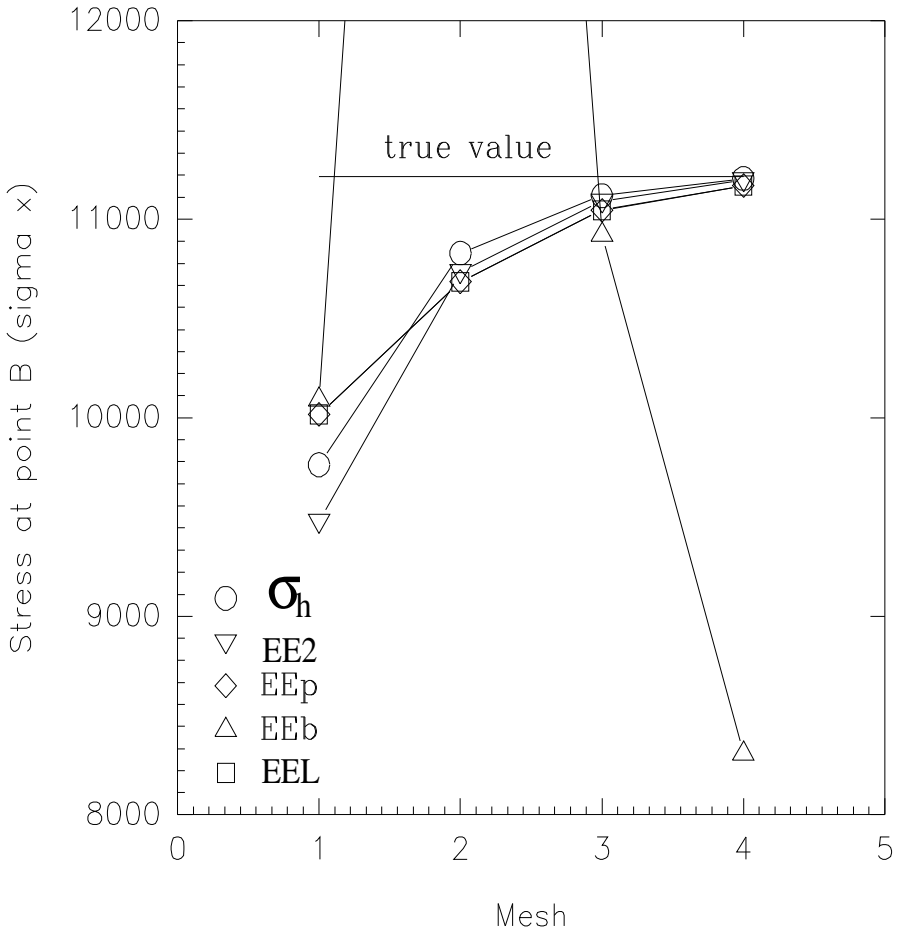

(a) σ_x at point A

(b) σ_x at point B

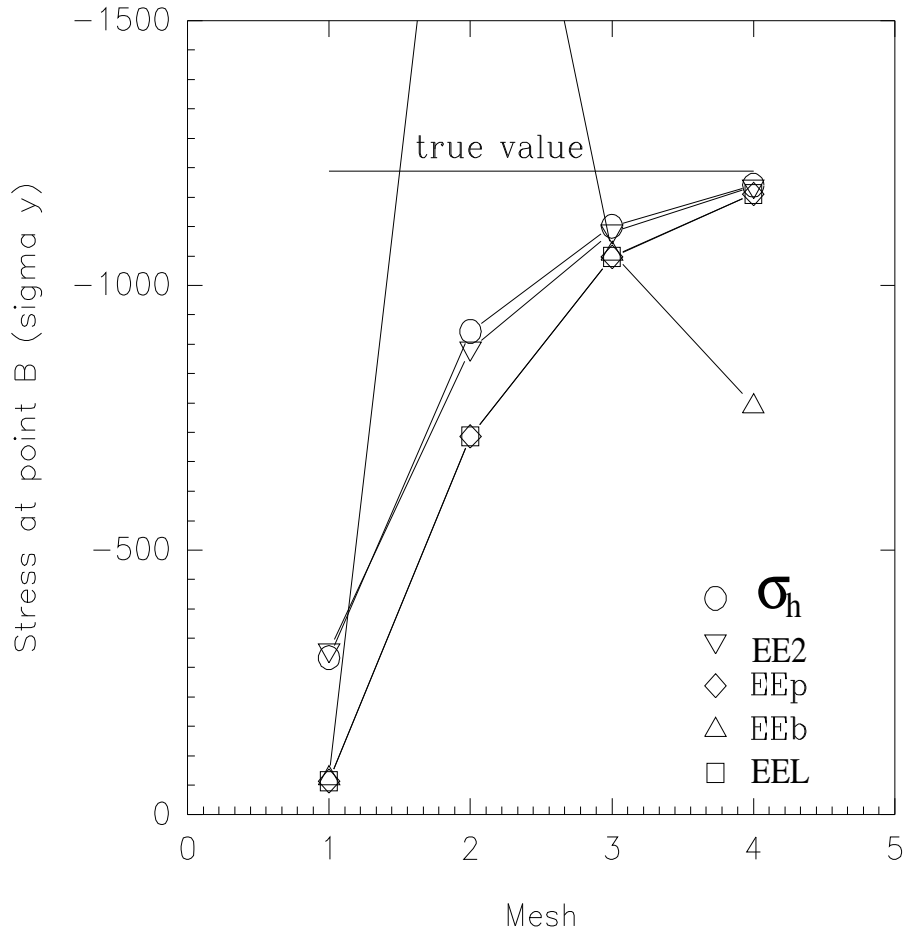
−1500
−1000
−500
0
Stress at point B (sigma y)
true value
0
1
2
3
4
5
Mesh
σh
EE2
EEp
EEb
EEL

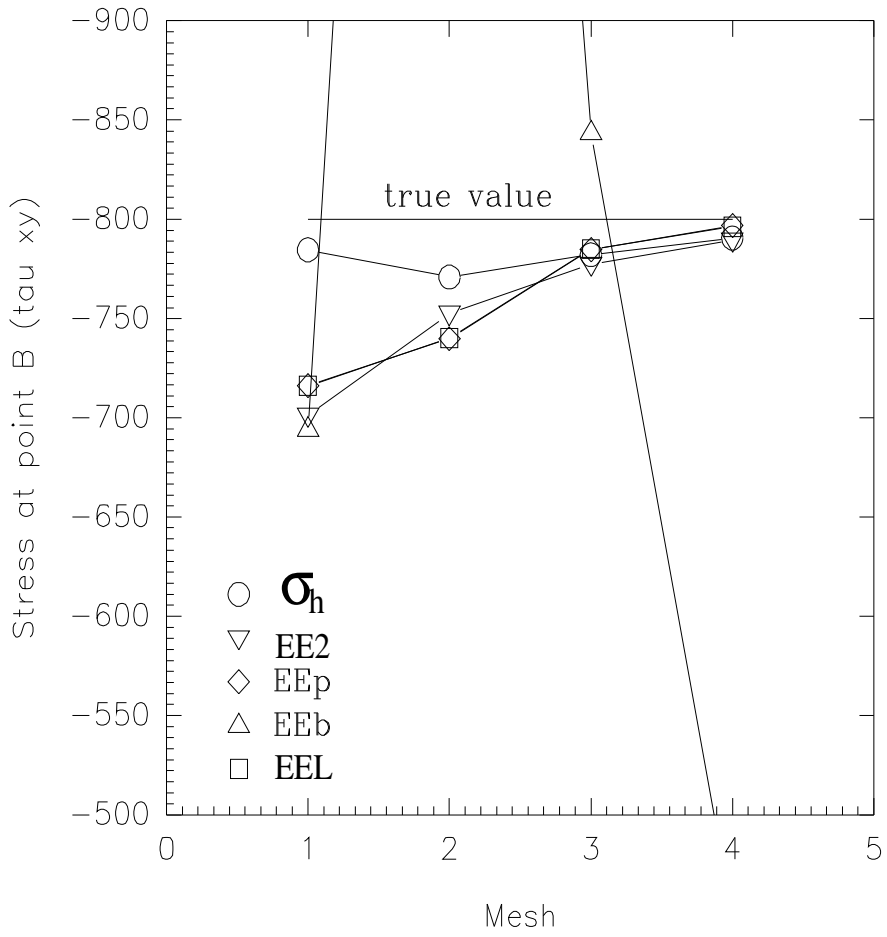

(c) σ_y at point B (d) τ_{xy} at point B

Figure 8. Convergence characteristics of error in recovered stress for Problem 2

The way in which the integrated quantities β and $\hat{U}$ converge for Problems 1 & 2 is shown in Table VI.

Table VI. Convergence of β and $\hat{U}$ for Problems 1 & 2. ($\hat{U}$ has units of *Nm*)

Problem	Mesh	β_2	β_L	β_b	β_p	$\hat{U}_2$	$\hat{U}_L$	$\hat{U}_b$	$\hat{U}_p$
1	1	0.710	0.710	0.710	0.710	103.73	30.13	30.13	30.13
	2	0.907	0.900	0.913	0.913	17.56	3.03	3.28	3.28
	3	0.972	0.969	0.972	0.972	2.341	0.256	0.281	0.281
	4	0.992	0.991	0.992	0.992	0.2933	0.0195	0.0211	0.0211
2	1	0.2768	1.3825	3.8637	1.5718	0.1498	0.3148	0.6412	0.2731
	2	0.4456	0.7521	3238.3	0.6814	0.0469	0.0526	171.67	0.0453
	3	0.5855	0.7831	9.3791	0.7358	0.0115	0.0097	0.157	0.0091
	4	0.7054	0.7974	398.06	0.7839	0.0023	0.0012	1.9318	0.0012

6. DISCUSSION OF RESULTS AND CONCLUDING REMARKS

An examination of the results for Problem 2 show clearly the effect of the problems associated with orientation dependence for EEb: the recovered stress at Point B and β and $\hat{U}$ tend to give rather exotic results (Reference 6 gives a clear account of the reasons for this phenomenon). By comparing these results with those for EEp it is seen that the use of the parent patch concept removes these problems.

In terms of the integrated measures β it is seen for Problem 1 that all error estimators considered are virtually as effective as each other. However, in terms of $\hat{U}$ it is seen that those error estimators employing a patch recovery scheme have estimated stress fields that are significantly closer to the exact one than EE2.

For Problem 2 it is observed that, for those error estimators using a patch recovery scheme the error estimation for Mesh 1 is poor. The reason for this lies in the fact that for this mesh all nodal stresses are recovered from a single patch. For subsequent meshes it is seen that the effectivity of these error estimators is better than that for EE2. In terms of $\hat{U}$ it is seen that whilst for Meshes 1 and 2 $\hat{U}_2 < \hat{U}_p < \hat{U}_L$, for Meshes 3 and 4 EEL and EEp perform better than EE2 with, for Mesh 4, $\hat{U}_p = \hat{U}_L \approx \frac{1}{2}\hat{U}_2$.

Turning now to the quality of the recovered stress at the chosen points of interest we observe that:

i) for Problem 1, although as the mesh is refined the difference becomes small, $\tilde{\boldsymbol{\sigma}}_2$ is closer to the true value than those recovered using a patch recovery scheme i.e. than $\tilde{\boldsymbol{\sigma}}_L$, $\tilde{\boldsymbol{\sigma}}_b$ and $\tilde{\boldsymbol{\sigma}}_p$. For all error estimators the rates of convergence of the recovered stresses are virtually identical with superconvergence observed only for internal nodes.

ii) for Problem 2 the quality of the recovered stress at the point of stress concentration (Point A) is strongly dependent on the scheme used to recover the stress[9]. It is seen that at this point the patch recovery schemes fair badly with the $\tilde{\boldsymbol{\sigma}}_2$ being significantly closer to the true value than $\tilde{\boldsymbol{\sigma}}_L$, $\tilde{\boldsymbol{\sigma}}_b$ and $\tilde{\boldsymbol{\sigma}}_p$. It is noted also that the basic finite element value σ_h (evaluated directly at the node) is the closest of all values.

Thus three conclusions are made:

i) if one wishes to use a bi-linear polynomial stress surface then the problem associated with orientation dependence can be avoided through the use of the parent patch concept. However, as the results presented have shown, although there is a difference in the results between EEL and EEp this difference is small and, therefore, one might be tempted to recommend the use of a linear polynomial stress surface.

ii) the results show that in terms of the effectivity ratio those error estimators employing a patch recovery scheme are equally or more effective than those using simple nodal averaging. In an integrated sense ($\hat{U}$) the estimated stress field resulting from a patch recovery scheme can be significantly nearer to the exact stress field than that resulting from simple nodal averaging.

iii) although, in general, the estimated stress field resulting from a patch recovery scheme may be superior to that achieved by simple nodal averaging, this is not always the case for point values c.f. Point A in Problem 2.

REFERENCES

1. O.C. Zienkiewicz & J.Z. Zhu, 'A Simple Error Estimator and Adaptive Procedure for Practical Engineering Analysis', Int. J. Num. Methods in Eng. **24**, 337-357 (1987).

2. O.C. Zienkiewicz & J.Z. Zhu 'Superconvergent Derivative Recovery Techniques and A Posteriori Error Estimation in the Finite Element Method Part I: A General Superconvergent Recovery Technique', Int. J. Num. Methods in Eng. **33**, 1331-1364 (1992).

3. J. Robinson, E.A.W. Maunder & A.C.A. Ramsay, 'Some Studies of Simple Error Estimators', A series of six articles in FEN, Issue No. 5 (1992) - Issue No. 3 (1993).

4. J. Barlow, 'Optimal Stress Location in FEM', Int. J. Num. Methods in Eng. Vol. 10, 243-251 (1976).

5. O.C. Zienkiewicz, J.Z. Zhu & J. Wu, 'Superconvergent Patch Recovery Techniques - Some Further Tests', Communications in Num. Methods in Eng. **9**, 251-258 (1993).

6. A.C.A. Ramsay & H. Sbresny, 'Some Studies of an Error Estimator Based on a Patch Recovery Scheme', A series of two articles in FEN, Issue No. 2 (1994) - Issue No. 4 (1994).

7. E.A.W. Maunder, 'Interpreting Stress Outputs from the "Standard" Four-Node Quadrilateral', FEN, Issue No.2, (1989).

8. B. Szabo & I. Babuska, 'Finite Element Analysis', John Wiley & Sons, (1991)

9. R.T. Tenchev, 'Accuracy of Stress Recovering and a Criterion for Mesh Refinement in Areas of Stress Concentration', FEN, Issue No.5 (1991).

10. O.C. Zienkiewicz & J.Z. Zhu, 'The Superconvergent Patch Recovery (SPR) and Adaptive Finite Element Refinement', Comp. Meth. in App. Mech. and Eng. 101, p207-224 (1992).